

Kick and Catch

Cooperative Microactuators for Freely Moving Platforms

INTRODUCTION

Microtechnology knows no ball bearings and therefore, deploys compliant structural connections instead. These connections limit an actuators range of motion. To bypass this constraint, an innovative design that omits all mechanical links has been proposed [1]. The “Kick and Catch”-project develops a similar multistable actuator system [2] featuring a freely moving component as illustrated in Fig. 1. This system deploys four electrostatic beam actuators, each utilizing electrostatic pull-in and mechanical leverage. Closed-loop control is inevitable for precise operation and an appropriate controller depends on efficient system-level models. This work aims to develop such an efficient system-level model based on multiphysical finite element models by means of model order reduction.

MODEL DESCRIPTION

A half of a single electrostatic beam actuator is modeled with finite elements as shown in Fig. 2. The geometry can be divided into three parts: a long tip to maximize leverage, a wide electrode for electrostatic actuation, and a meander spring for structural connection. The perforation pattern is required for etching processes and additionally reduces squeeze film damping. The complete structure is made from a silicon wafer and material data was assigned considering its crystal lattice. The electrostatic actuation causes a pull-in motion of the beam, generating considerable force magnitudes. This load case is analyzed within a static, nonlinear finite element simulation. The nonlinearities drastically increase computational demand and originate from electrostatic forces. Such a force acts on every of the electrode’s 2759 finite element nodes and has the form:

$$F_{el,i} = -\frac{1}{2} \varepsilon A_i (gap_{0,i} + u_{z,i})^{-2} U^2. \quad (1)$$

The force’s magnitude depends on the electrode’s initial gap $gap_{0,i}$, the node’s vertical displacement $u_{z,i}$, its effective area A_i , the permittivity ε , and the voltage applied to the electrode U . The finite element model contains 2759 of these nonlinear forces which are computed in numerous iterations.

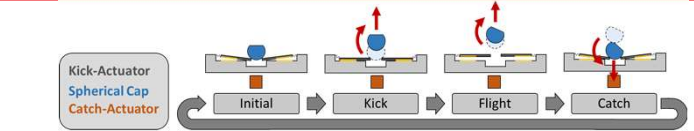


Fig. 1. Working principle of the microactuator developed within the DFG-funded “Kick and Catch”-project: The four electrostatic kick actuators transfer momentum to the hemisphere and thus, launch it into a free-flight phase. An electromagnetic catch actuator controls the motion and allows for an actively damped landing back on the kick-actuator. This procedure results in a rotated hemisphere in a stable resting position. Repeating these steps allows for high deflection.

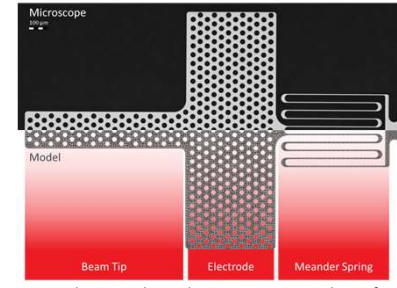


Fig. 2. Electromechanical microactuator and its finite element model. The upper half shows a manufactured silicon beam with a total length of ca. 2 mm and meander structures of $5 \mu\text{m}$ thickness. The lower half presents the finite element model of this design which translates into a system of 25.134 second-order ordinary differential equations.

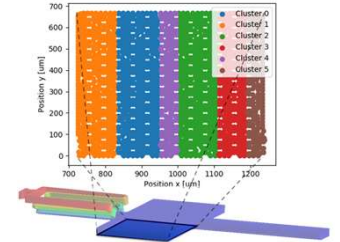


Fig. 3. The nonlinear term $(gap_{0,i} + u_{z,i})^{-2}$ is evaluated for each node i and scaled by its term $-\frac{1}{2} \varepsilon A_i$. To reduce the number of nonlinear evaluations, a clustering algorithm groups the electrode’s nodes by their vertical displacement. Hence, the term $(gap_{0,i} + u_{z,i})^{-2}$ is only evaluated for each of the six clusters but still scaled node-wise.

MODEL ORDER REDUCTION

Original Model

The finite element model shown in Fig. 2 corresponds to a system of second-order ordinary differential equations of the form:

$$\sum \left\{ \begin{array}{l} \mathbf{M} \cdot \ddot{\mathbf{x}}(t) + \mathbf{E} \cdot \dot{\mathbf{x}}(t) + \mathbf{K} \cdot \mathbf{x}(t) = \mathbf{B} \cdot \mathbf{u}(t) + \mathbf{f}_{el}(\mathbf{x}(t), U(t)) \\ \mathbf{y}(t) = \mathbf{C} \cdot \mathbf{x}(t) \end{array} \right. , \quad (2)$$

where $\mathbf{M}, \mathbf{E}, \mathbf{K} \in \mathbb{R}^{N \times N}$ are the system’s mass matrix and damping matrix. $\mathbf{B} \in \mathbb{R}^{N \times m}$ distributes the loads from the input vector $\mathbf{u}(t) \in \mathbb{R}^m$ and $\mathbf{C} \in \mathbb{R}^{p \times N}$ computes the output vector $\mathbf{y}(t) \in \mathbb{R}^p$ based on the state vector $\mathbf{x}(t) \in \mathbb{R}^N$. N , m , and p are the number of degrees of freedom, inputs, and user-defined outputs, respectively. $\mathbf{f}_{el}(\mathbf{x}(t), U(t)) \in \mathbb{R}^{p \times N}$ contains the $p_{NL} = 2759$ nonlinear displacement-dependent forces in the form of Eq. (1).

Model Order Reduction

Eq. (2) accurately describes the actuator’s behavior but at high computational costs. Krylov subspace-based model order reduction generates a surrogate model of drastically smaller dimension as indicated in Fig. 4. This step projects the system in Eq. (2) onto a low-dimensional subspace $V \in \mathbb{R}^{N \times n}$ and results in the reduced system

$$\sum_r \left\{ \begin{array}{l} \frac{V^T \mathbf{M} \mathbf{V}}{M_r} \cdot \ddot{\mathbf{x}}_r(t) + \frac{V^T \mathbf{E} \mathbf{V}}{E_r} \cdot \dot{\mathbf{x}}_r(t) + \frac{V^T \mathbf{K} \mathbf{V}}{K_r} \cdot \mathbf{x}_r(t) = \frac{V^T \mathbf{B}}{B_r} \cdot \mathbf{u} + V^T \mathbf{f}_{el}(V \cdot \mathbf{x}_r, U) \\ \mathbf{y}(t) = \frac{C \mathbf{V}}{C_r} \cdot \mathbf{x}_r(t) \end{array} \right. , \quad (3)$$

where M_r, E_r, K_r, B_r , and C_r are the reduced system matrices of corresponding dimensions. Although $n = 120 \ll N = 25.134$, simulating this system is not drastically faster than the original system in Eq. (2) due to the nonlinear term $V^T \mathbf{f}_{el}(V \cdot \mathbf{x}_r, U)$.

Clustering Nonlinearities

To accelerate the nonlinear evaluations, they are approximated by computing only a small subset. An agglomerative clustering algorithm determines the six best subsets as indicated in Fig. 3. As a result, a total of six nonlinearities is evaluated and subsequently distributed, resulting in a highly efficient reduced order model.

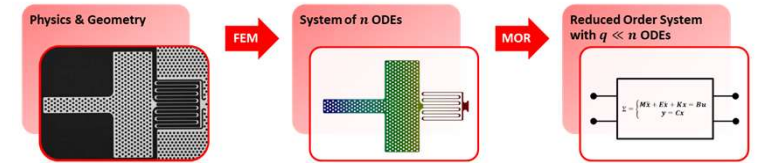


Fig. 4. Schematic workflow of model order reduction illustrated for the electrostatic actuator. The electrostatic actuator is modeled via FEM. Subsequently, projection-based MOR drastically reduces the system’s dimension while maintaining very high accuracy.

Simulation Results

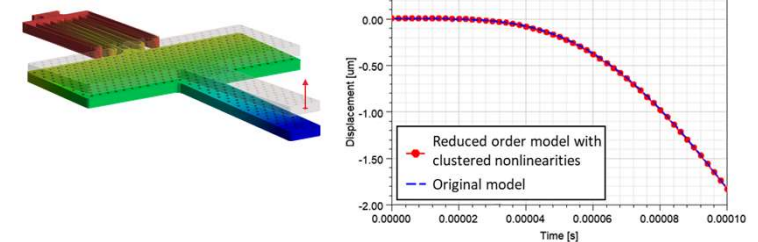


Fig. 5. Results of a transient analysis of the microactuator when actuated with $U = 70 \text{ V}$ for $1e - 4 \text{ s}$. The quantity shown is the vertical displacement of the beam’s tip as shown on the left. The two solutions are computed by the original model and by the reduced order model. Note that the initial system with dimension 25134 and 2759 nonlinearities has been reduced to a dimension of 200 and six nonlinear forces.

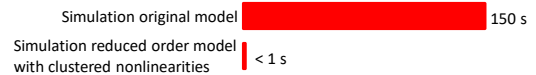


Fig. 6. Comparing the computational solution time between the original model in Eq. (2) and the reduced order model with clustered nonlinearities (6 x AMD Ryzen™ 5 3600 @ 3,6 GHz, 16 GB RAM).

CONCLUSIONS

- We present the reduction of a weakly nonlinear system in combination with clustering nonlinearities for an electromechanical microactuator.
- This combined method demonstrates excellent accuracy and superior computational efficiency.
- In contrast to existing methods for grouping, the clustering process relies on numerical results instead of heuristics.

LITERATURE

- [1] F. Bunge, S. Leopold, S. Bohm, and M. Hoffmann, “Scanning micromirror for large, quasi-static 2D-deflections based on electrostatic driven rotation of a hemisphere”, In *Sensors and Actuators A: Physical*, Vol. 243, pp. 159-166, 2016.
- [2] M. Farny and M. Hoffmann, “Kick & Catch: elektrostatisches Rotieren einer Kugel,” in *MikroSystemTechnik Kongress*, Stuttgart-Ludwigsburg: VDE Verlag GmbH, pp. 274–277, 2021.
- [3] L. Del Tin, “Reduced-order modelling, circuit-level design and SOI fabrication of microelectromechanical resonators,” Università di Bologna, 2007.

